

Damage assessment of beams from changes in natural frequencies using ant colony optimization

Aditi Majumdar¹, Ambar De², Damodar Maity² and Dipak Kumar Maiti*¹

¹Department of Aerospace Engineering, Indian Institute of Technology, Kharagpur-721302, India

²Department of Civil Engineering, Indian Institute of Technology, Kharagpur-721302, India

(Received June 21, 2011, Revised October 22, 2012, Accepted January 6, 2013)

Abstract. A numerical method is presented here to detect and assess structural damages from changes in natural frequencies using Ant Colony Optimization (ACO) algorithm. It is possible to formulate the inverse problem in terms of optimization and then to utilize a solution technique employing ACO to assess the damage/damages of structures using natural frequencies. The laboratory tested data has been used to verify the proposed algorithm. The study indicates the potentiality of the developed code to solve a wide range of inverse identification problems in a systematic manner. The developed code is used to assess damages of beam like structures using a first few natural frequencies. The outcomes of the simulated results show that the developed method can detect and estimate the amount of damages with satisfactory precision.

Keywords: ant colony optimization; damage assessment; inverse problem; finite element method; natural frequency; stiffness reduction factor

1. Introduction

The damage detection technologies and evaluation of their residual life of structure are very important to assure the structural integrity of operating plants and structures. Damage may be caused under service conditions due to limited fatigue strength. They may also be due to mechanical defects. Some of the damages, which are inside the material, are developed as a result of manufacturing processes. Sometimes the extent and location of damage can be determined through visual inspection. But visual inspection technique has a limited capacity to detect damage, especially when damage lies inside the structure and is not visible from outside. So an effective and reliable damage assessment methodology will be a valuable tool in timely determination of damage and deterioration state of structural element.

Modal parameters based analysis has several advantages over alternative techniques due to the fact that the modal parameters depend only on the mechanical characteristics of the structure and not on the excitation applied. Frequencies can be measured more easily than mode shapes and as a result they are less affected by experimental errors. In damage detection problem two objectives have to be attained; the location of damage and its magnitude or severity. From the changes in

*Corresponding author, Associate Professor, E-mail: dkmaiti@aero.iitkgp.ernet.in

natural frequencies the inverse problem related to damage detection may be formulated to determine the location and percentage of damage.

One class of damage location and assessment procedure, which has attracted considerable interest in recent years, is based on the alternation of the vibration characteristics of structures due to damage. Sanayei and Onipede (1991) presented a method to detect damage, which is simulated through stiffness reduction under static load. For this method, applied force and measured displacement should be at same DOF in the structure. Wu *et al.* (1992) used the pattern matching capability of a neural network to recognize the location and the extent of damage of individual member from the measured frequency spectrum of the damage structure. Mares and Surace (1996) described a technique to identify the location and quantification of the extent of the damage with genetic algorithms, by using the residual force method, which is based on the conventional modal analysis theory. Nikolakopoulos *et al.* (1997) showed the dependency of the first two structural eigen frequencies on crack depth and location by the use of contour graph form. To identify the location and depth of a crack in a framed structure, one only needs to determine the intersecting point of the superposed contours that correspondence to measured eigen frequency variations caused by the pressure of crack. Ruotolo and Surace (1997) used the modal parameters of the lower modes for the non-destructive detection and sizing of cracks in beams. They used a finite element model of the structure to calculate the dynamic behavior. The damage detection problem is formulated in optimization sense employing genetic algorithm. Cerri and Vestroni (2000) addressed the problem of identifying structural damage using measured frequencies. The beam model has a damaged zone in which the stiffness is lower than that of the undamaged value. Morassi (2001) presented a method, which deals with the identification of a single crack in a vibrating rod based on the knowledge of the damage – induced shifts in a pair of natural frequencies. Liu and Chen (2002) proposed a computational inverse technique for identifying stiffness distribution on structures using structural dynamics response in the frequency domain. Tripathy and Maity (2004) used curvature damage factor as a possible candidate for the damage identification by back propagation neural network algorithm. Maity and Saha (2004) proposed neural network technique to detect damage through response measurement of structures. They applied the idea on a simple cantilever beam where strain and displacement are used as possible candidates for damage identification by a back-propagation neural network. Maity and Tripathy (2005) used the genetic algorithm to detect and assess the structural damage from changes in natural frequencies. They formulate the inverse problem in optimization form and then to utilize a solution procedure with genetic algorithm to assess the damage. Sahoo and Maity (2007) proposed a hybrid neuro-genetic algorithm in order to automate the design of neural network for different type of structures. They considered the frequencies and strains as input parameters and the location and amount of damage as output parameters. Beena and Ganguli (2010) developed a new fuzzy cognitive map (FCM) algorithm to detect damaged location in structures. They used the continuum mechanics approach as a stiffness reduction and also represented the accuracy of FCM with respect to the numerical results. Vallabhaneni and Maity (2011) developed an algorithm using radial basis neural network considering curvature damage factor for assessing damages in structures and showed the efficacy over the well known back propagation neural network algorithm.

Ant colony optimization (ACO) is used for computational hard problems by emulating the natural behaviors of ants. In the literature several application of ACO like traveling salesman problem (TSP), vehicle routing problems are addressed. Shyu *et al.* (2004) proposed the ACO to a two – machine flow shop scheduling problem. They developed ACO algorithm with several

specific features and compare with others heuristic algorithm. The numerical results reveal that the ACO algorithm exhibits impressive performances with small error. Bell and McMullen (2004) used ACO for vehicle routing problems (VRP). They presented the experimental data which shows that the algorithm is successful in finding solutions within 1% of known optimal solutions and the use of multiple ant colonies is found to provide a comparatively competitive solution technique especially for larger problems. Meziane *et al.* (2005) used ACO for reliability based optimization under performance and cost constraints to determine the optimal electrical power network topology. Kaveh *et al.* (2008) proposed ACO for topology optimization of 2D and 3D structures. Their aim was to find the stiffest structure with a certain amount of material, based on the element's contribution to the strain energy. The ACO algorithm provides a suitable tool to handle the problem as an on-off discrete optimization. Kaveh *et al.* (2009) used ACO to formulate null based on triangular plane stress and plane strain finite element models corresponding to highly sparse and banded flexibility matrices. The efficiency of their proposed method is illustrated with numerical examples. Kaveh *et al.* (2010) presented a performance-based optimal seismic design of framed structures using the ACO method. They developed the algorithm which is simple computer-based method for push-over analysis which accounts for first-order elastic and second-order geometric stiffness properties. They used the nonlinear analysis to arrive at the structural response at various seismic performance levels.

From the previous research work, it is understood that damage may be detected in better way if natural frequency is considered as the structural response. Some of the researchers have used neural network for damage detection, which has many disadvantages like difficulty to train the network, solution converges to local minima, etc. A robust damage assessment methodology must be capable of recognizing patterns in the observed response of the structure resulting from individual member damage including the capacity of determining the extent of damage. In the past few years, heuristic algorithms, such as ant colony algorithms, have found many applications in optimization problems. In the present research study, ACO technique is proposed in damage detection of structures. The aim is to formulate an objective function in terms of parameters related to the physical properties and state of the structure. The objective function must be formulated in such a way that the minimum value is obtained when evaluated with the true parameters. The stiffness reduction factor (SRF), which is considered as design variable for each element, is used to evaluate the objective function in the present formulation. Each factor corresponds to the reduction in the stiffness of one of the elements from which the structure is composed as compared to the counterpart in the integral (undamaged) structure. The lower and upper values of SRFs are considered as design constraints. The objective function incorporates response parameter which being evaluated in terms of damaged stiffness matrix. In the present research study the beam problems are considered for demonstration purpose to show the effectiveness of the present algorithm for various damage cases. The laboratory tested data are also used to establish the accuracy of the proposed technique.

2. Ant colony optimization

Ant colony optimization algorithms are models inspired by the behavior of ant colonies. Studies have been made to show how ants, which are almost blind, are capable of finding the shortest paths from their nests to feeding sources and back. This behavior is due to ants' capacity for transmitting information between themselves, through a pheromone trail along the chosen path.

In this way, while an isolated ant moves essentially at random, the “agents” of an ant colony detect the pheromone trail left by other ants and tend to follow that trail. These ants then deposit their own pheromone along the path, thus reinforcing it and making it more attractive. It can thus be said that the process is characterized by a positive feedback loop, in which the probability of an ant choosing a path increases with the number of ants which have previously used the same path.

Many of the practical problems are hard. They may not be solved to optimal solution within polynomially bounded computational domain. Hence, to solve practically large instances, one has to use approximate methods, known as heuristics, which return near-optimal results. ACO is a metaheuristic in which a colony of artificial ants cooperates in finding good solutions to difficult discrete optimization problems. Cooperation is a key design component of ACO algorithms. The choice is to allocate the computational resources to a set of relatively simple agents (artificial ants) that communicate indirectly by stigmergy, i.e., by indirect communication mediated by the environment. Good solutions are an emergent property of the agents’ cooperative interactions.

An artificial ant in ACO is a stochastic procedure that incrementally builds a solution under construction. Therefore, the ACO metaheuristic can be applied to any combinatorial optimization problem for which a constructive heuristic can be defined. Thus, while applying ACO, the real issue is how to map the considered problem to a representation that can be used by the artificial ants to build solutions. The principles of ACO in detail may be found in Dorigo and Stutzle (2004). The flowchart of the ACO is shown in FIG. 1.

2.1 Problem representation

In order to apply ACO, a minimization problem of (S, f, Ω) is considered, where S is the set of candidate solutions, f is the objective function which assigns an objective value $f(s, t)$ to each candidate solution $s \in S$ and $\Omega(t)$ is a set of constraints. The parameter t indicates that the objective function and the constraints can be time-dependent, as in case, for example, in applications to dynamic problems. The goal is to find a globally optimal feasible solution s^* , that is, a minimum cost feasible solution to the minimization problem. The combinatorial optimization problem (S, f, Ω) is mapped on a problem that can be characterized by the following list of items: (a) A finite set $C = \{c_1, c_2, \dots, c_{Nc}\}$ of components, where Nc is used to represent a finite set of elements, (b) The states of the problem are defined in terms of sequences $x = \langle c_i, c_j, \dots, c_h \dots \rangle$ of finite length over the elements of C , the set of all possible states is denoted by χ . The length of a sequence x , that is, the number of components in the sequence, expressed by $|x|$. The maximum length of a sequence is bounded by a positive constant $n < +\infty$. (c) The set of (candidate) solutions S is a subset of χ . (d) A set of feasible states $\tilde{\chi}$, with $\tilde{\chi}$ being a sub-set of χ , defined via a problem-dependent test that verifies that it is not impossible to complete a sequence $x \in \tilde{\chi}$ into a solution satisfying the constraints Ω . (e) A non-empty set S^* of optimal solutions, with S^* being a sub-set of both $\tilde{\chi}$ and S . (f) A cost $g(s, t)$ is associated with each candidate solution $s \in S$.

Given this formulation, artificial ants build solutions by performing randomized walks on the completely connected graph $G_c = (C, L)$ whose nodes are the components C , and the set L fully connects the components C . The graph G_c is called constructive graph and the elements of L are called connections.

2.2 Ant’s behavior

In ACO algorithms artificial ants are stochastic constructive procedures that build solutions by

moving on the construction graph $G_c = (C, L)$, where the set L fully connects the components C . The problem constraints $\Omega(t)$ are built into the ants' constructive heuristic. In most applications, ants construct feasible solutions. Components $c_i \in C$ and connections $l_{ij} \in L$ can have an associated pheromone trail τ and a heuristic value η . The pheromone trails encode a long term memory about the entire ant search process, and is updated by the ants themselves.

Each ant k of the colony has the following properties: (a) It exploits the graph $G_c = (C, L)$ to search for optimal solutions $s^* \in S^*$. (b) It has a memory M^k that it can use to store information about the path it followed so far, and it used to build feasible solutions, compute the heuristic values η , evaluate the solution found and retrace the path backward. (c) It has a start state x_s^k and one or more termination conditions e^k . (d) When in state $x_r = \langle x_{r-1}, i \rangle$, if no termination conditions are satisfied, it moves to a node j in the neighborhood $N^k(x_r)$, that is, to a state $\langle x_r, j \rangle \in \chi$. If at least one of the termination conditions are satisfied, then the ant stops. When an ant builds a candidate solution, moves to infeasible states are forbidden in most applications, either through the use of the ant's memory, or via appropriately defined heuristic values η . (e) It selects a move applying a probabilistic decision rule. The probabilistic decision rule is a function of the locally available pheromone trails and heuristic values, the ant's private memory storing its current state, and the problem constraints. (f) When adding a component c_j to the current state, it can update the pheromone trail τ associated with it or with the corresponding connection. (g) Once it has built a solution, it can retrace the same path backward and update the pheromone trails of the used components.

2.3 Ant searching behavior

Suppose an ant k , when located at a node i , uses the pheromone trail τ_{ij} . One may compute the probability of its choosing j as the next node as

$$p_{ij}^{(k)} = \begin{cases} \frac{\tau_{ij}^\alpha}{\sum_{j \in N_i^{(k)}} \tau_{ij}^\alpha} & \text{if } j \in N_i^{(k)} \\ 0 & \text{if } j \notin N_i^{(k)} \end{cases} \quad (1)$$

where α denotes the degree of importance of the pheromones and $N_i^{(k)}$ indicates the set of neighborhood nodes of ant k when located at node i . The neighborhood of node i contains all the nodes directly connected to node i except the preceding node.

2.4 Path retracing and pheromone updating

The k^{th} ant deposits $\Delta\tau^{(k)}$ of pheromone on arcs before returning to the home node (backward node). The pheromone value τ_{ij} on the arc (i, j) traversed is updated as follows

$$\tau_{ij} \leftarrow \tau_{ij} + \Delta\tau^{(k)} \quad (2)$$

The probability of this arc being selected by the forthcoming ants will increase by the increase of pheromone.

2.5 Pheromone trail evaporation

When an ant k moves to the next node, the pheromone evaporates from all the arcs i, j according to the relation

$$\tau_{ij} \leftarrow (1 - \rho) \tau_{ij}; \forall (i, j) \in A \quad (3)$$

where $\rho \in [0, 1]$ is the pheromone evaporation rate (also known as the pheromone decay factor) and A denotes the segments or arcs traveled by the ant k in its path from home to the destination. After all the ants return to the home node (nest), the pheromone information is updated according to the relation

$$\tau_{ij} = (1 - \rho)\tau_{ij} + \sum_{k=1}^N \Delta\tau_{ij}^{(k)} \quad (4)$$

Where, $\Delta\tau_{ij}^{(k)}$ is the amount of pheromone deposited on arc i, j by the best ant k . The goal of pheromone update is to increase the pheromone value associated with good or promising paths. The pheromone deposited on arc i, j by the best ant is taken as

$$\Delta\tau_{ij}^{(k)} = \frac{Q}{L_k} \quad (5)$$

Here Q is a constant and L_k is the length of the path traveled by the ant k . The above expression can be implemented as

$$\Delta\tau_{ij}^{(k)} = \begin{cases} \zeta f_{best} & \text{if } (i, j) \in \text{global best tour} \\ f_{worst} & \\ 0; & \text{otherwise} \end{cases} \quad (6)$$

where f_{worst} is the worst value and f_{best} is the best value of the objective function among the paths taken by the N ants, and ζ is a parameter used to control the scale of the global updating of the pheromone. The larger the value of the pheromone deposited on the global best path, the better the exploitation ability. The aim of Eqs. (3), (6) is to provide a greater amount of pheromone to the tours (solutions) with better objective function values. Considering these aspects, the pheromone decay factor (ρ) is assumed to be 0.5 and ζ to be 0.99.

The objective function constructed for this research study is the difference between the frequency of the damaged beam and the beam being considered under the ACO algorithm. It is considered that when the frequency difference is lower and the pheromone deposit will be higher then there is a high probability of the damage being in the considered element. Finally, the beam element/elements with the highest pheromone concentration (in mathematical sense the highest probability) is/are having damage.

3. Finite element formulation

In this section displacement based finite element formulation is described in brief.

3.1 The element matrices of beam

The dynamic response of a structure may be derived by minimizing the work of internal, inertial and viscous forces for any small kinematically admissible motion. Using Hamilton's principle for dynamic problems, we can write

$$\int_{t_1}^{t_2} (T - V) dt = 0 \tag{7}$$

Where T is the total kinetic energy of the system and V is the potential energy of the applied forces. The variable t represents time dimension. Using q_1, q_2, \dots, q_n as the generalized coordinates and assuming they are independent, the Euler-Lagrange equations then yield well-known *Lagrange* equation of motion, given as follows in terms of the Lagrangian $L = T - V$

$$\frac{d}{dt} \left(\frac{\partial L}{\partial \dot{q}_i} \right) - \frac{\partial L}{\partial q_i} = 0 \quad i = 1, 2, \dots, n \tag{8}$$

To develop Hamilton's principle for continua from the method of virtual work, D'Alembert principle is employed, which sets forth Newton's second law. For a continuous deformable body, the inertia force for the D'Alembert principle is given as $-\rho \cdot d^2u/dt^2$ and is force acting over the entire body. A virtual displacement field δu_i at a particular time instant t for a dynamic system can be represented as follows

$$-\iiint_V \rho \frac{d^2 u_i}{dt^2} \delta u_i dv + \iiint_V B_i \delta u_i dv + \iint_S T_i^{(v)} \delta u_i dS = \iiint_V \tau_{ij} \delta \epsilon_{ij} dv \tag{10}$$

The force potential V may be represented as follows

$$V = -\iiint_V B_i u_i dv - \iint_S T_i^{(v)} u_i dS \tag{11}$$

Where B_i and $T_i^{(v)}$ are the external body loads such that there is overall equilibrium for the body from the viewpoint of rigid body mechanics. The forces B_i and $T_i^{(v)}$ are assumed to be statically compatible. Having included the effect of point loads $\{p\}_i$, Eq. (3) may be expressed in matrix form as follows

$$-\iiint_V \rho \{\delta u\}^T \{\ddot{u}\} dv + \iiint_V \{\delta u\}^T \{b\} dv + \iint_S \{\delta u\}^T \{T\} dA + \sum_{i=1}^n \{\delta u_i\}^T \{p\}_i = \iiint_V \{\delta \epsilon\}^T [\sigma] dv \tag{12}$$

The formulation to include energy dissipation introduces the term δW_{diss} which is as follows

$$\delta W_{diss} = \delta \left(\iiint_V \{u\}^T \{f\} dv \right) \tag{13}$$

where $\{f\}$ is the dissipation force vector per unit volume. For the case of viscous damping $\{f\}$ is proportional to the velocity. Therefore, it can be said

$$\{f\} = c \{\dot{u}\} \tag{14}$$

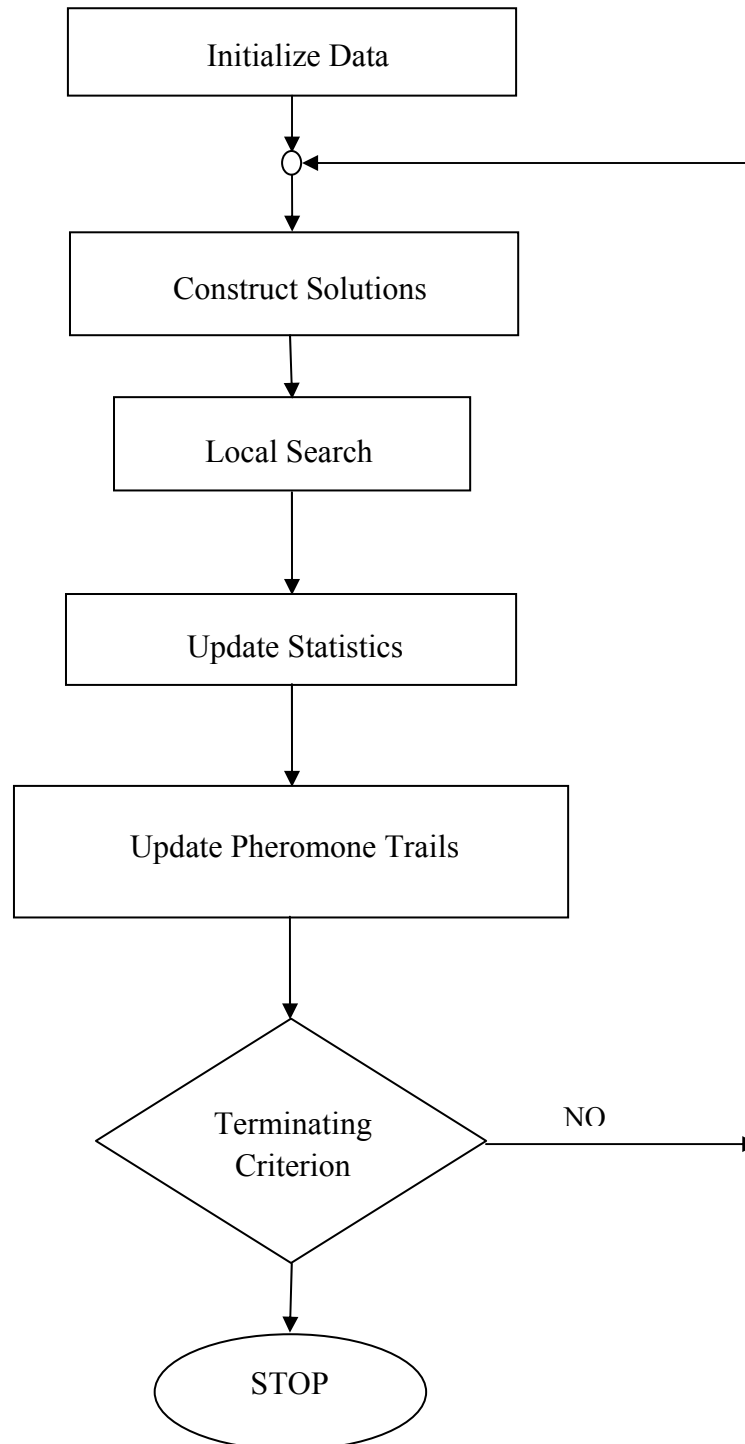


Fig. 1 Flowchart of ACO

After dividing the body into small finite elements and considering the displacement field $\{u\}$ as a function of nodal displacements $\{q\}$ and interpolation functions N_i , we have

$$u = N_i q_i \tag{15}$$

Also, the spatial coordinate of any point inside the body is expressed in terms of each nodal coordinates as follows

$$x = N_i x_i \tag{16}$$

The strain field $\{\varepsilon\}$ and the stress field $\{\sigma\}$ are expressed as follows

$$\{\varepsilon\} = [B]\{q\} \tag{17}$$

$$\{\sigma\} = [D]\{\varepsilon\} \tag{18}$$

By including the viscous damping, Eq. (5) can be expressed as follows

$$\begin{aligned} & - \iiint_V \{\delta q\}^T [N]^T [N] \{\ddot{q}\} dv + \iiint_V \{\delta q\}^T [N]^T \{b\} dv + \iint_S \{\delta q\}^T [N]^T \{T\} dA \\ & + \sum_{i=1}^n \{\delta q\}^T \{p\}_i - \iiint_V \{\delta q\}^T [N]^T c [N] \{\dot{q}\} dv = \iiint_V \{\delta q\}^T [B]^T [D][B] dv \end{aligned} \tag{19}$$

Eq. (12) may be written in the following manner

$$\{\delta q\}^T ([K]\{q\} + [M]\{\ddot{q}\} + [C]\{\dot{q}\}) = \{\delta q\}^T \{f\} \tag{20}$$

Where

$$[K] = \iiint_V [B]^T [D][B] dv \tag{21}$$

$$[M] = \iiint_V [N]^T \rho [N] \{\ddot{q}\} dv \tag{22}$$

$$[C] = \iiint_V [N]^T c [N] \{\dot{q}\} dv \tag{23}$$

$$\{f\} = \iiint_V [N]^T \{b\} dv + \iint_S [N]^T \{T\} dA + \sum_{i=1}^n \{\delta u_i\}^T \{p\}_i \tag{24}$$

The matrices $[K]$, $[M]$, $[C]$ and $\{f\}$ represents stiffness, mass, damping matrices and force vector respectively. Finally, the dynamic equation of equilibrium may be expressed as follows

$$[M]\{\ddot{q}\} + [C]\{\dot{q}\} + [K]\{q\} = \{f\} \tag{25}$$

where $\{q\}$, $\{\dot{q}\}$ and $\{\ddot{q}\}$ denotes the displacement, velocity and acceleration of any point inside the structural body. The vector $\{f\}$ represents the applied external forces on the structure. For free vibration analysis, the above expression can be simplified in the following form by neglecting damping terms and considering no external forces.

$$[M]\{\ddot{q}\} + [K]\{q\} = \{0\} \tag{26}$$

As the structure in the present case is beam, the element stiffness and mass matrix will be as follows

$$[k] = \int_0^L [B]^T EI_z [B] dx = \frac{EI_z}{L^3} \begin{bmatrix} 12 & 6L & -12 & 6L \\ 6L & 4L^2 & -6L & 2L^2 \\ -12 & -6L & 12 & -6L \\ 6L & 2L^2 & -6L & 4L^2 \end{bmatrix} \quad (27)$$

$$[m] = \frac{\rho AL}{420} \begin{bmatrix} 156 & 22L & 54 & -13L \\ 22L & 4L^2 & 13L & -3L^2 \\ 54 & 13L & 156 & -22L \\ -13L & -3L^2 & -22L & 4L^2 \end{bmatrix} \quad (28)$$

3.2 Damage formulation

Damage is considered as reduction in stiffness only, without any change in mass of the structure. To incorporate this, a parameter 'stiffness reduction factor' (SRF) is introduced. Each factor corresponds to the reduction in stiffness of one of the elements from which the structure is composed as compared to the integral structure. This parameter is used in all our further study to indicate damage. When damage occurs in a structure, the stiffness matrix of the damaged structure, denoted as $[k_d]$ can be expressed as the sum of element stiffness matrix multiplied by the SRF β_i ($i = 1, 2, \dots, m$) associated with each of the m elements. i.e

$$[k_d] = \sum_i (1 - \beta_i) [k_i] \quad (29)$$

where $\beta_i = EI_u^i - EI_d^i / EI_u^i$

Here E is defined as Young's modulus of elasticity and I is the moment of inertia and the subscript u & d denotes the undamaged and damaged states respectively, and β is the stiffness reduction factor. The percentage of damage is considered as 0% to 60%. Therefore the values of β_i ranges from 0 to 0.6. The j^{th} eigen value equation associated with the above equation is

$$[K_d] \{\phi_j\} - \lambda_j [M] \{\phi_j\} = 0 \quad (30)$$

where λ_j is the eigen value and $\{\phi_j\}$ is the corresponding normalized eigen vector.

The mass matrix $[M]$ is unaltered even in the damaged condition. Also the natural frequencies and mode shapes of the damaged structure continues to satisfy the eigen value equation. The j^{th} mode of such damaged structure therefore satisfies the equation

$$[K_d] \{\phi_{jd}\} - \lambda_{jd} [M] \{\phi_{jd}\} = \{0\} \quad (31)$$

The problem of damage detection is basically a constrained nonlinear optimization problem, where the stiffness reduction factor for each element is defined as the updating parameters. The usual approach to solve this problem is to minimize an objective function, which is defined in terms of discrepancies between the vibration data identified by modal testing and those computed

from the analytical model. Accordingly, the objective function used for this study is given by

$$F = \sqrt{\frac{1}{n} \sum_{i=1}^n \left(\left(\frac{f_i^m}{f_i^c} \right) - 1 \right)^2} \quad (32)$$

Where, f_i^m and f_i^c are the frequencies obtained from finite element simulation and the frequency obtained from optimization iteration steps respectively. n is the number of input response parameters (natural frequencies) and for this study is taken as 6.

4. Results and discussions

The computer codes developed in the present study based on the formulation outlined in the previous sections are applied on beam type structural system. The calculated first three or first six natural frequencies are used as input response. The damage is defined as a reduction in stiffness of the element. In the present study, damages at single location as well as multiple locations in the structures are considered for the present study. The pheromone evaporation rate is assumed to be 0.5 for all cases.

4.1 Validation of the proposed algorithm

The laboratory tested data of first three natural frequencies without and with damage of the cantilever beam is presented in Table 1. The experimental values are used here to test the algorithm presented in the foregoing section. The configuration of the experimental study was a cantilever beam of length 530 mm, width 25 mm and depth 6 mm as shown in Fig. 2(a). The beam was made of steel with Young's modulus of $200 \times 10^9 \text{ N.m}^{-2}$ and mass density of 7800 kg.m^{-3} . The beam was damaged by a saw cut having the depth 2 mm and width 1.8 mm as shown in Fig. 2(b).

The beam is modeled by 20 equal / unequal Euler – Bernoulli beam elements and first three natural frequencies are calculated by eigen value analysis and are listed in Table 2. The damage is introduced by reducing its stiffness in element number 4 in the FE model while calculating the natural frequencies in the damaged beam as given in the Fig. 2(b). The deviation of computational natural frequencies with those of experimental one can be attributed to inherent uncertainties of the material, geometry effects from the end support or measurement error, noise etc. It is observed from the FE analysis that the natural frequencies predicted by FE code are well within the accepted range. The variation is observed with 5% – 6% deviation with respect to experimental results. The damaged natural frequencies of the beam are listed in Table 2. It is observed that the percentage variations with undamaged state employing FE model closely match with those of experimental results. This proves the accuracy of the FE analysis.

The second part of the above analysis is to detect the damage through ACO when damaged and undamaged natural frequencies are given as input response to the ACO algorithm. In the initial step the possible damaged combinations are generated through ACO algorithm. The iteration steps will converge to a most probable path of damage to minimize the difference between damaged input frequencies to those of computed frequencies through ACO. The update natural frequencies are listed in column 5 of Table 2 with the application of ACO. It is observed that the predicted damaged natural frequencies closely match with those of the input frequencies.

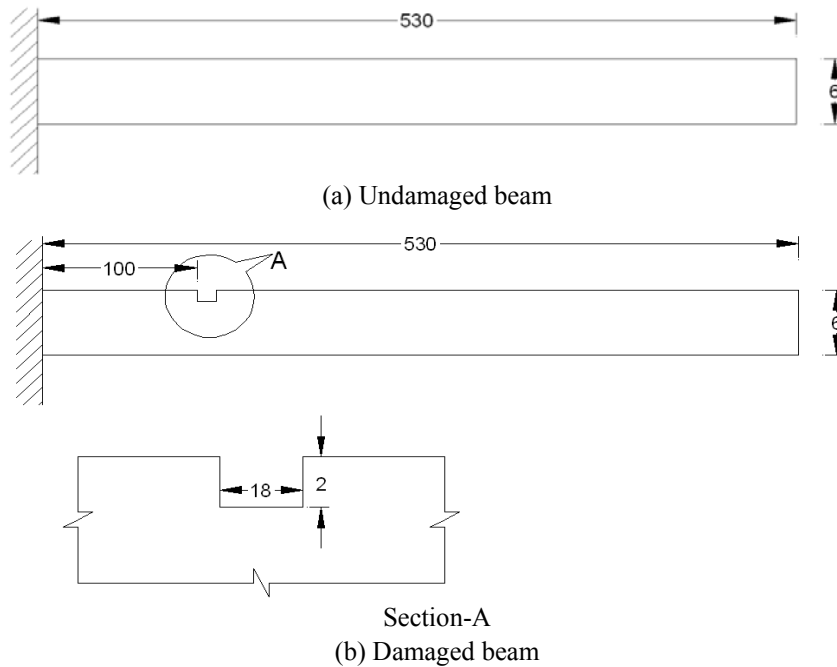


Fig. 2 Steel cantilever beam (All dimensions are in mm)

Table 1 Experimental frequencies of cantilever beam (Hz)

Mode	Undamaged state	Damaged state	% Variation with respect to undamaged state
1	16.41	16.25	0.97
2	103.63	103.99	-0.347
3	290.0	289.52	0.166

Table 2 Frequencies of cantilever beam (Hz) from FE model

Mode	FE result (Undamaged)	% variation with respect to experimental undamaged state	Damaged beam	Update state using ACO (Damaged)	% Deviation with ACO w.r.t. FE Damaged results
1	17.3973	6.01	17.23	17.25	0.86
2	109.2783	5.45	109.65	109.27	-0.33
3	306.2965	5.61	305.79	303.552	0.90

A convergence study has been carried out to determine the optimal no. of ants for the algorithm. 80% damage has been introduced by reducing the stiffness of element 4. Damage as predicted by ACO is shown in Table 3. Three cases have been considered by varying no of ants 50, 100 and 150. When no of ants increased from 100 to 150 the increase in accuracy is very negligible. Therefore, for subsequent study the no of ants consider is taken as 100.

Table 3 Convergence study with no. of ants

No. of Ant	Predicted damaged element along with damage percentage	
	with first three natural frequencies	with first six natural frequencies
50	4@77.39	4@77.56
100	4@77.85	4@78.33
150	4@77.86	4@78.33

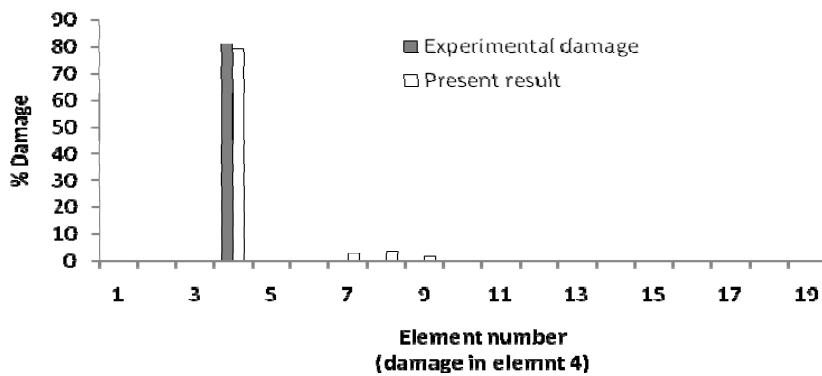
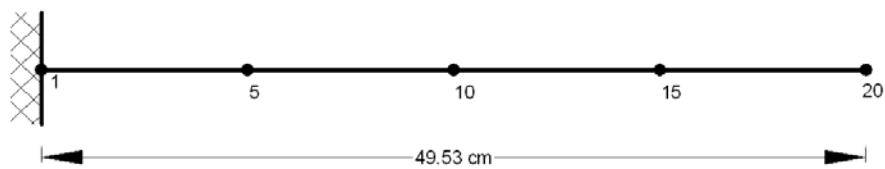


Fig. 3 Comparison of result on damage identification of a cantilever beam

Fig. 3 shows the results obtained by the present method for the identification of the damage along with the experimental frequencies. It is observed from the results that the actual damage is detected successfully. It is observed from Fig. 3 that there is small quantity of pseudo damage present in the output. That is due to numerical error.

4.2 Damage on a cantilever beam

A simple cantilever beam is considered in the present analysis to demonstrate the efficiency and robustness of the developed algorithm. The dimensions and material properties of the beam are considered same as taken in section 4.1. The beam (Fig. 4) is discretized with 20 elements. The first three or six natural frequencies are calculated and used in the objective function for a comparison of the result.



$$b = 2.54 \text{ cm}, d = 0.635 \text{ cm}, E = 7.1 \times 10^7 \text{ KPa}, \rho = 2210 \text{ kg.m}^{-3}$$

Fig. 4 Cantilever beam problem

4.2.1 Case 1: cantilever beam with single element damage

For the single damage (element 9) two parameters are considered in this case. The first one is with the first three natural frequencies and the second one with first six natural frequencies for a comparison. The comparison of probability of damage with number of element is shown in Fig. 5 for first three and first six natural frequencies. It is clear from Fig. 5 that damage probability is high in element number 9. The comparison of the output (Fig. 6) shows that the damage may be assessed more accurately while first six frequencies are used as input instead of first three frequencies. The variations of objective function with number of iteration are shown in Fig. 7 and Fig. 8 for first three and six natural frequencies respectively.

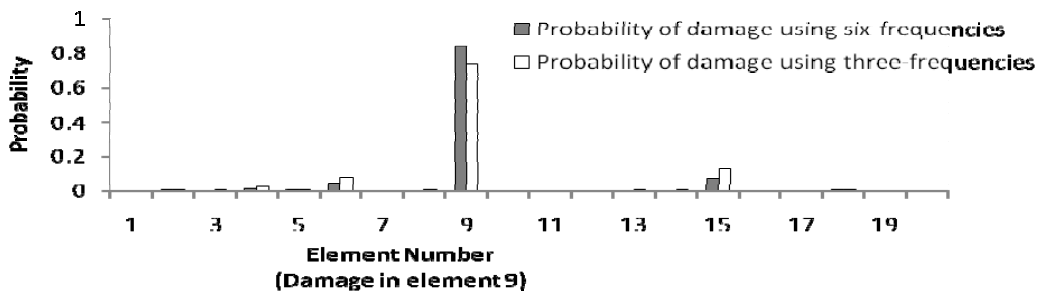


Fig. 5 Probability of damage in various elements considering first three and six frequencies

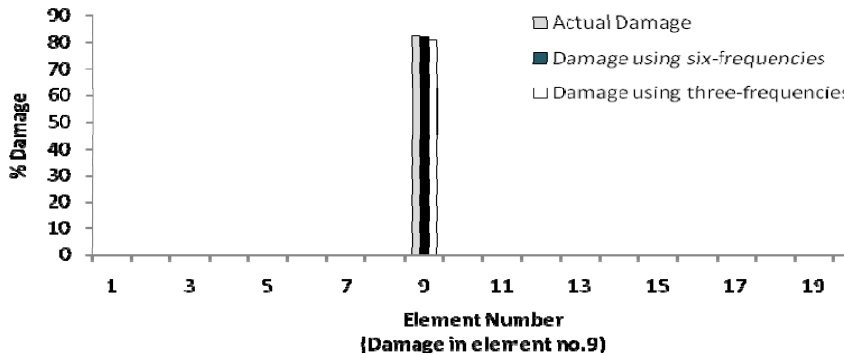


Fig. 6 Comparison of assessment of damage using first three and six frequencies

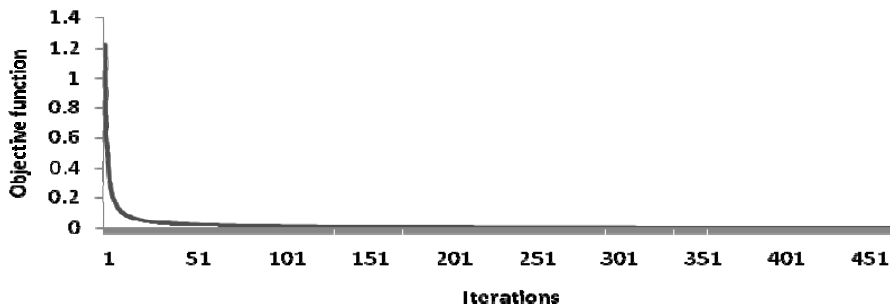


Fig. 7 Variation of objective function with no. of iteration using first three frequencies

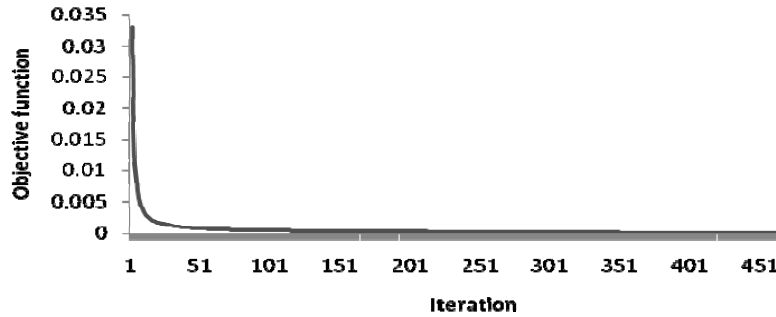


Fig. 8 Variation of objective function with no. of iteration using first six frequencies

Table 4 Summary of ACO output with variation of location and amount of damage for a cantilever beam

Element @ % damage	Using three frequencies	Error %	Using six frequencies	Error %
2@20%	2@19.17%	4.15	2@19.37%	3.15
2@40%	2@39.14%	2.15	2@39.23%	1.92
2@60%	2@59.42%	0.97	2@59.62%	0.63
9@20%	9@19.23%	3.85	9@19.38%	3.1
9@40%	9@39.04%	2.4	9@39.10%	2.25
9@60%	9@59.31%	1.15	9@59.41%	0.98

The parametric study is performed to assess the capability of the present algorithm to detect various amount of damage. The damages of amount 20%, 40% and 60% have been introduced in 2nd and 9th elements for single damage case. The damages percentages as calculated by the algorithm are tabulated in Table 4. It is found that the proposed algorithm could correctly detect the number of damage and amount of damage very close to the exact one.

4.2.2 Case 2: cantilever beam with two element damage

In this case damage in two elements i.e., element number 5 and 15 have been simulated using first three and first six natural frequencies. The comparison of probability with number of elements is shown in Fig. 9 for first three and first six natural frequencies. The output results (Fig. 10) show that the damage may be assessed with better accuracy in this case as well while first six frequencies are used as input instead of first three frequencies.

The parametric study is also performed with two elements damage. The damages amounting 20%, 40%, 60% and 80% have been introduced in element 5 and 15. The algorithm has run with 100 ants and up to 500 iterations. The damages percentages as calculated by the algorithm are tabulated in Table 5. It is found that the proposed algorithm could correctly detect the damaged element even with the presence of multiple damages close to the exact one.

4.3 Damage on a two span continuous beam

A two equal span continuous beam as shown in Fig. 11 is considered to study the efficacy of

the present algorithm. The length, width and depth of each span are considered as 24.765 cm, 2.54 cm and 0.635 cm respectively. The material properties of the beam are considered same as considered in section 4.1. The first three and six natural frequencies are calculated and used the probability study for the effectiveness of the proposed algorithm.

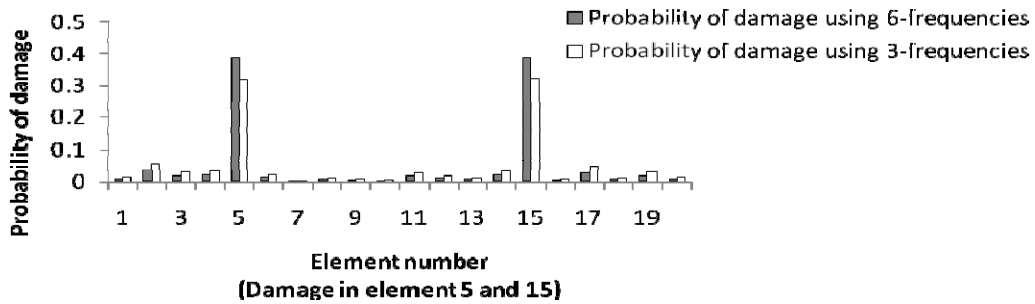


Fig. 9 Probability of damage in various element considering first three and six frequencies

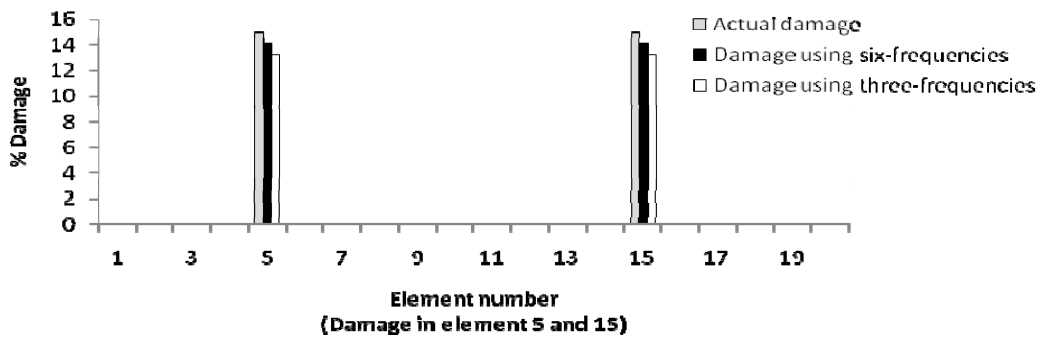


Fig. 10 Comparison of assessment of damage using first three and six frequencies

Table 5 Summary of ACO prediction with variation of amount of damage with two elements combinations

Element @ % damage	ACO prediction using three frequencies	ACO prediction using six frequencies
5@20%, 15@20%	5@19.17%, 15@19.15%	5@19.21%, 15@19.22%
5@40% , 15@40%	5@39.11%, 15@39.09%	5@39.19% , 15@39.17%
5@60% , 15@60%	5@59.30% , 15@59.21%	5@59.42% , 15@59.32%
5@80% ,15@80%	5@79.37% ,15@79.34%	5@79.58% , 15@79.57%

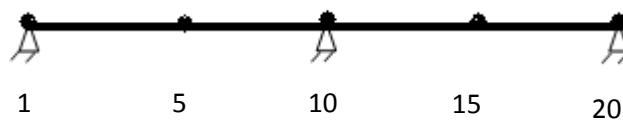


Fig. 11 Two span beam

4.3.1 Case 1: continuous beam with single element damage

First three and six natural frequencies are considered in this case as well to study the effectiveness of the developed code. The comparison of probability with number of element is shown in Fig. 12 for first three and first six natural frequencies. It is clear from Fig. 12 that damage probability is high in element number 9. The comparison of the output (Fig. 13) shows that the damage may be assessed with higher degree of accuracy while first six frequencies are used as input instead of first three frequencies. However, use of natural frequency alone may give misleading result for detecting damage in symmetric location as the response may be the same for alternative cases. The variations of the objective function with number of iterations are shown in Fig. 14 and Fig. 15 for first three natural frequencies and first six natural frequencies respectively.

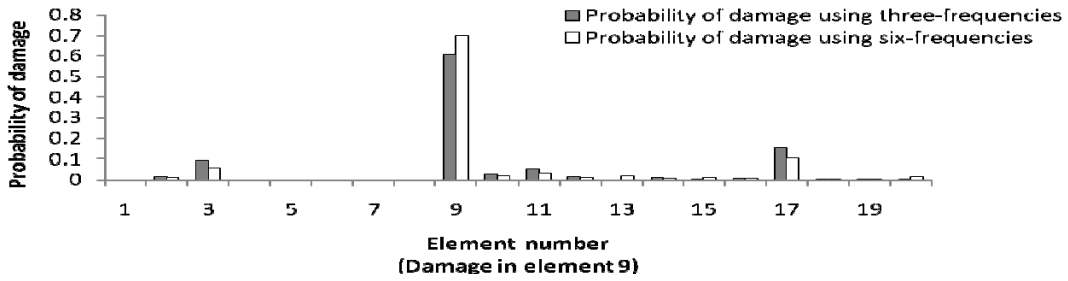


Fig. 12 Probability of damage in various element considering first three and six frequencies

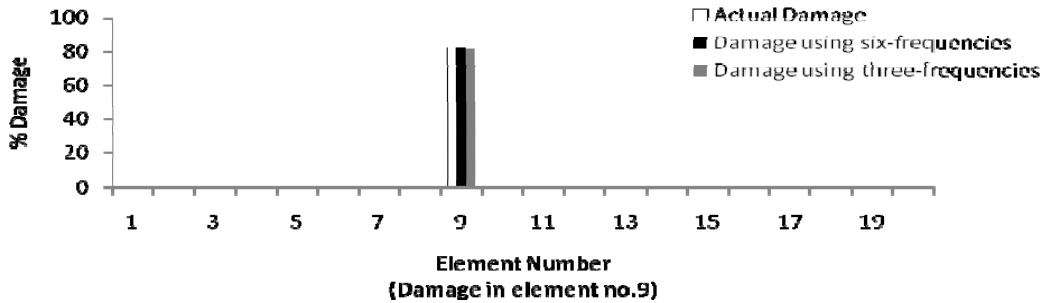


Fig. 13 Comparison of assessment of damage using first three and six frequencies

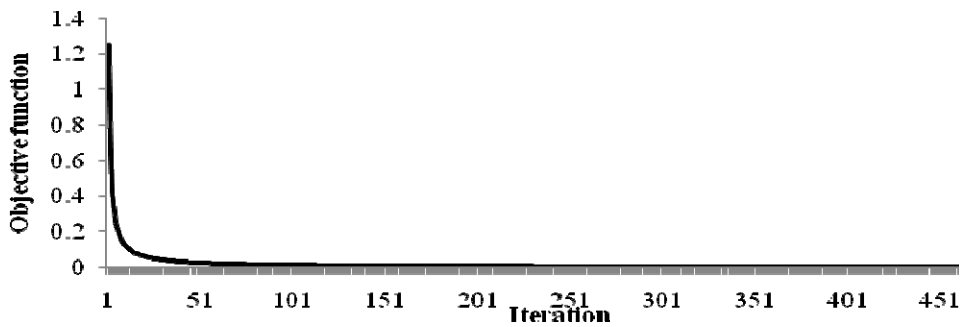


Fig. 14 Variation of objective function with no. of iteration using first three frequencies

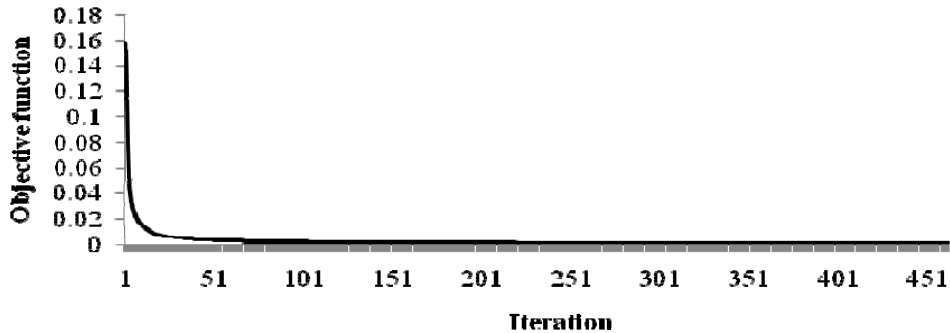


Fig. 15 Variation of objective function with no. of iteration using first six frequencies

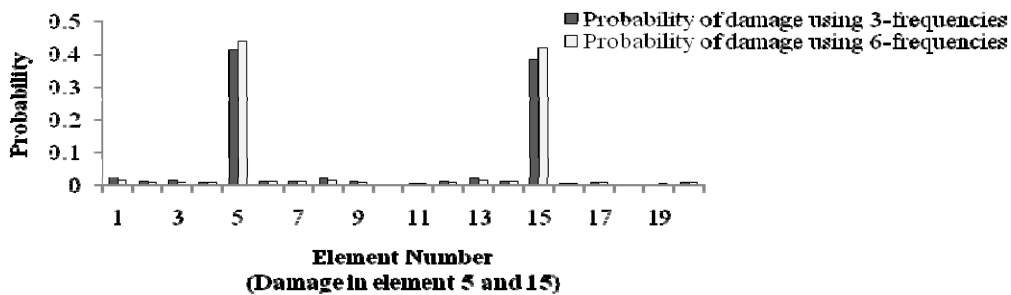


Fig. 16 Probability of damage in various element considering first three and six frequencies

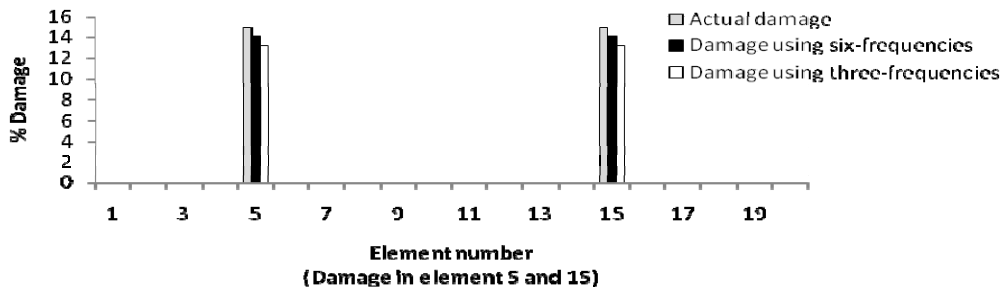


Fig. 17 Comparison of assessment of damage using first three and six frequencies

4.3.2 Case 2: two span beam with two element damage

Damages in two elements i.e., element number 5 and 15 have been simulated using first three and first six natural frequencies for two continuous beam also. The comparison of probability of damages in various elements is shown in Fig. 16 using first three and first six natural frequencies. The simulated results (Fig. 17) show that the damage can be assessed more accurately while first six frequencies are used as input in place of first three frequencies.

The damage has been introduced in various elements with variation in amount of damage to check the efficiency of proposed algorithm as shown in Table 6. 20%, 40%, 60% and 80% damages have considered for the present study. The results from ACO algorithm are found to be

quite satisfactory with correct detection of damaged element and the amount of damage percentage.

Table 6 Summary of introduced damages and its prediction by ACO algorithm

Element @ % damage	ACO prediction using three frequencies	ACO prediction using six frequencies
2@20%, 6@20%	2@19.18% , 6@19.15%	2@19.27%, 6@19.21%
3@40% , 5@40%	3@39.20% , 5@39.14%	3@39.26% , 5@39.16%
4@60% , 8@60%	4@59.28%, 8@59.20%	4@59.35% , 8@59.33%
7@80% ,11@80%	7@79.34% ,11@79.50%	7@79.46% ,11@79.58%

5. Conclusions

A simple but robust methodology is presented to determine the location and amount of damage in beam like structures using ant colony optimization algorithm. A laboratory tested data on cantilever beam has been used to validate the proposed technique, which shows the accuracy and efficiency of the present algorithm. The two different types of beams, i.e., cantilever beam and two span continuous beam, are considered in the present study to demonstrate the efficiency of the algorithm, although it can be used for all types of beam and support combinations. The most significant advantages of this method over the traditional search methods used for the inverse problems are that this algorithm is much faster and gives much more accurate results. Care has been taken to avoid local maxima and the initial imperfect pheromone depositions leading to preferential building of concentration to sub-optimal results. As indicated by the test results, the accuracy increases with the increase in number of measured natural frequencies. However, it has been found that the first three natural frequencies may be sufficient enough to detect the location of the damage/damages.

References

- Beena, P. and Ganguli, R. (2010), "Structural damage detection using fuzzy cognitive maps and hebbian learning", *Applied Soft Computing*, **11**, 1014 - 1020.
- Bell, E.J. and McMullen, R.P. (2004), "Ant colony optimization techniques for the vehicle routing problem", *Advanced Engineering Informatics*, **18**, 41-48
- Cerri, N.M. and Vestroni, F. (2000), "Detection of damage in beams subjected to diffused cracking", *J. Sound Vibration*, **234**, 259-276.
- Dorigo, M. and Stutzle, T. (2004), *Ant colony optimization*, The MIT Press, Cambridge, Massachusetts, London, England.
- Kaveh, A. and Daei, M. (2009), "Efficient force method for the analysis of finite element models comprising of triangular elements using ant colony optimization", *Finite Elements in Analysis and Design*, **45**, 710-720.
- Kaveh, A., Farahmand, B.A., Hadidi, A., Sorochi, F.R. and Talatahari, S. (2010), "Performance-based seismic design of steel frames using ant colony optimization", *Journal of Constructional Steel Research*, **66**(4), 566-574.

- Kaveh, A., Hassani, B., Shojaei, B. and Tavakkoli, M.S. (2008), "Structural topology optimization using ant colony methodology", *Computers and Structures*, **86**, 1539-1549.
- Liu, R.G. and Chen, C.S. (2002), "A novel technique for inverse identification of distributed stiffness factor in structures", *J. Struct. Eng.*, **254**, 823-835.
- Maity, D. and Saha, A. (2004), "Damage assessment in structure from changes in static parameter using neural networks", *Sadhana, Journal of the Indian Academy of Sciences*, **29**, 315-327.
- Maity, D. and Tripathy, R.R. (2005), "Damage assessment of structure from changes in natural frequencies using genetic algorithm", *Structural Engineering and Mechanics*, **19**, 21-42.
- Mares, C. and Surace, C. (1996), "An application of genetic algorithms to identify damage in elastic structures", *J. Sound Vibration*, **195**, 195-215.
- Meziane, R., Massim, Y., Zeblah, A., Ghoraf, A. and Rahli, R. (2005), "Reliability optimization using ant colony algorithm under performance and cost constraints", *Electric Power Systems Research*, **76**, 1-8.
- Morassi, A. (2001), "Identification of a crack in a rod based on changes in a pair of natural frequencies", *J. Sound Vibration*, **242**, 577-596.
- Nikolakopoulos, P., Katsareas, D. and Papadopoulos, C. (1997), "Crack identification in frame structures", *J. Computer Structure*, **64**, 389-406.
- Ruotolo, R. and Surace, C. (1997), "Damage assessment of multiple cracked beams: Numerical results and experimental validation", *J. Sound Vibration*, **206**, 567-588.
- Sahoo, B. and Maity, D. (2007), "Damage assessment of structures using hybrid neuro-genetic algorithm", *Applied Soft Computing*, **7**, 89-104.
- Sanayei, M. and Onipede, O. (1991), "Damage assessment of structure using static test data", *AIAA*, **29**, 1174-1179.
- Shyu, S.J., Lin, T.M.B. and Yin, Y.P. (2004), "Application of ant colony optimization for no-wait flowshop scheduling problem to minimize the total completion time", *Computer & Industrial Engineering*, **47**, 181-193.
- Tripathy, R.R. and Maity, D. (2004), "Damage assessment of structures from changes its curvature damage factor using artificial neural network", *Indian J. of Engineering & material Science*, **11**, 369-377.
- Vallabhaneni, V. and Maity, D. (2011), "Application of Radial Basis Neural Network on Damage Assessment of Structures", *Procedia Engineering*, **14**, 3104 - 3110.
- Wu, X., Ghaboussi, J. and Garrett, H.J. (1992), "Use of neural networks in detection of structural damage", *Computer Structure*, **42**, 649-659.